



ISSN: 0067-2904

GIF: 0.851

Determination the Heating Rate and the Characteristic Age for Pulsars Stars

Sundus A. Abdulla Albakri*, Hasanain H. Al-dahlaki, Talib Abd-Almalik

Department of Astronomy and Space, College of Science, University of Baghdad, Baghdad, Iraq

Abstract

Pulsar stars are rotating Neutron stars can be divided into two types Millisecond and Normal Pulsars. In this work the magnetic field are concentrated depends on the period (P), and Period derivative (\dot{P}) for a sample Normal, Millisecond and Radio stars which adopted. In addition, the values of spin down luminosity and Heating rate are determined by depending on (Ostriker and Gunn) model. The results showed that older Millisecond define as having greater ages specified how long pulsars lives at that ages very long period pulsars to be observable have particularly large surface magnetic field. The results indicate that spin down of luminosity for Millisecond and Normal star must due to the main energy loss rotation axis to align with magnetic axis as pulsar age. In addition, the Heating rate decreases with the star's age, beside Characteristic age calculated.

Keywords: Pulsar, Neutron stars, Magnetic field, MSP Pulsars.

تعيين نسبة التسخين والعمر المميز للنجوم النابضة

سندس عبد العباس عبد الله البكري*, حسنين حسن علي، طالب عبد الملك

قسم الفلك والفضاء، كلية العلوم، جامعة بغداد. بغداد، العراق

الخلاصة

النجوم النابضة هي نجوم نيوترونية دوارة تقسم إلى قسمين هي نوع الملي ثانية والاعتيادية. في هذا البحث تم التركيز على تأثير المجال المغناطيسي اعتماداً على فترة الدورات (P) ومشتقة الفترة (\dot{P}) لعينة من نجوم الاعتيادية والملي ثانية والراديو. بالإضافة إلى ذلك تم تعيين قيم تباطؤ اللعانية ونسبة التسخين بالاعتماد على نموذج (Ostriker and Gunn). النتائج أوضحت أن النجوم من نوع ملي الثانية القديمة التكوين هي تملك أعظم عمر مميز حيث يمكن وصف ان هذه النجوم هي التي تملك اطول فترات زمنية دورانية نابضة حيث يمكن رصدها عملياً بمجال مغناطيسي اقلي عالي. بينت النتائج ايضاً ان تباطؤ اللعانية لنجوم الملي ثانية والنجوم الاعتيادية النابضة يرجع الى خسارة الطاقة حيث محور التدوير يميل الى ان ينطبق مع المحور المغناطيسي مع تقدم عمر النابض. نسبة التسخين تقل مع عمر النجم وكذلك تم حساب العمر المميز.

Introduction

A neutron star is a type of stellar remnant that can result from the gravitational collapse of a massive star during a Type II, Type Ib or Type Ic supernova event. Neutron stars are the densest and tiniest stars known to exist in the universe; although having only the diameter of about 10 km (6 mi), they

*Email: sundusalbakri7a@yahoo.com

may have a mass of several times that of the Sun. Neutron stars probably appear white to the naked eye [1].

Neutron stars are the end points of stars whose mass after nuclear burning is greater than the Chandrasekhar limit for white dwarfs, but whose mass is not great enough to overcome the neutron degeneracy pressure to become black holes.

Neutron stars are very hot and are supported against further collapse by quantum degeneracy pressure due to the phenomenon described by the Pauli Exclusion Principle. This principle states that no two neutrons (or any other fermionic particles) can occupy the same place and quantum state simultaneously [2]. Born in supernova explosions, these bodies are "only" ~12-13 kilometers by radius and spin around as rapidly as 642 times a second or approximately 38,500 revolutions per minute.

A typical neutron star has a mass between ~1.4 and 3.2 solar masses with a surface temperature of $\sim 6 \times 10^5$ Kelvin. In contrast, the Sun's radius is about 60,000 times that. Neutron stars have overall densities of 3.7×10^{17} to 5.9×10^{17} kg/m³ (2.6×10^{14} to 4.1×10^{14} times the density of the Sun) which is comparable to the approximate density of an atomic nucleus of 3×10^{17} kg/m³. The neutron star's density varies from below 1×10^9 kg/m³ in the crust - increasing with depth - to above 6×10^{17} or 8×10^{17} kg/m³ deeper inside. This density is approximately equivalent to the mass of a Boeing 747 compressed to the size of a small grain of sand. A normal-size of neutron star material would have a mass of approximately 5 billion tons as shown in figure 1 [3,4].

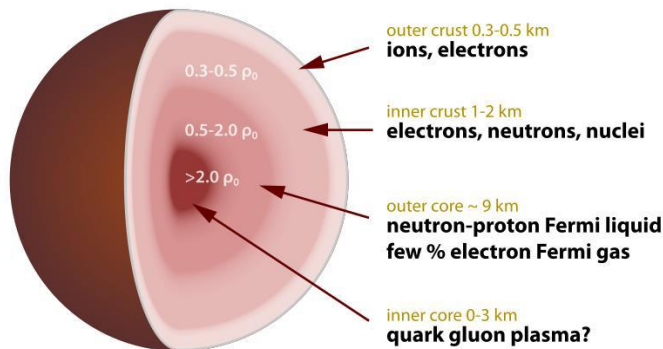


Figure 1- Represents the Cross-section of neutron star. Densities are in terms of the saturation nuclear matter density, where nucleons begin to touch [4].

The Difference between Millisecond and Normal Pulsars

At the time of the discovery of the first millisecond pulsar B1937+21 by Backer et.al. (1982), around 350 pulsars were known. While most of these had period of around 1s, the period of PSB1937+21 was a mere 1.2 ms, immediately raising the question of in what respect such object differs from long-period pulsar. Like the original binary pulsar, B1913+16, with a period of 59 ms, it was proposed that millisecond pulsars originate in binary systems. The differences for these pulsars can be estimated by the following [5]:

- ❖ Millisecond pulsar differs in evolutionary history from that of normal pulsars also differs in their radio emission properties and MSP spectra are significantly different from normal pulsar.
- ❖ MSP are also slightly less luminosity and less efficient radio emitters than normal pulsars [6,7].
- ❖ Finally, about 80% of all millisecond pulsars found in our galactic plane are member of binary systems [8].
- ❖ MSP rotate much faster than the Normal pulsar as the observation shows the results of the period time that may approach to less than 1ms [8].
- ❖ The surface magnetic field of MSP is much less than the Normal pulsars [9].
- ❖ The characteristic age of MSP is longer than the Normal pulsars because MSP consider very old stars.

The Magnetic Field

A magnetic field is a mathematical description of the magnetic influence of electric currents and magnetic materials. The magnetic field at any given point is specifying by both a direction and a magnitude (or strength); as such, it is a vector field as shown in figure 2a and figure 2b. The term is

use for two distinct but closely related fields denoted by the symbols B and H , which are measure in units of tesla and amp per meter respectively in the SI. B is most commonly defined in terms of the Lorentz force it exerts on moving electric charges [10].

Magnetic fields are produce by moving electric charges and the intrinsic magnetic moments of elementary particles associated with a fundamental quantum property, their spin. In special relativity, electric and magnetic fields are two interrelated aspects of a single object, called the electromagnetic tensor; the split of this tensor into electric and magnetic fields depends on the relative velocity of the observer and charge. In quantum physics, the electromagnetic field is quantize and electromagnetic interactions result from the exchange of photons [10].

The Earth produces its own magnetic field, which is important in navigation. Rotating magnetic fields are use in both electric motors and generators. Magnetic forces give information about the charge carriers in a material through the Hall Effect. The interaction of magnetic fields in electric devices such as transformers is study in the discipline of magnetic circuits [11].

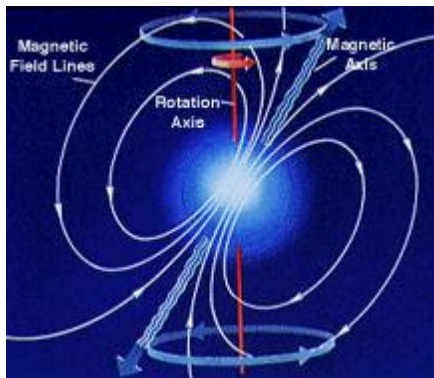


Figure 2-a- a diagram of a pulsar showing its rotation axis [11].

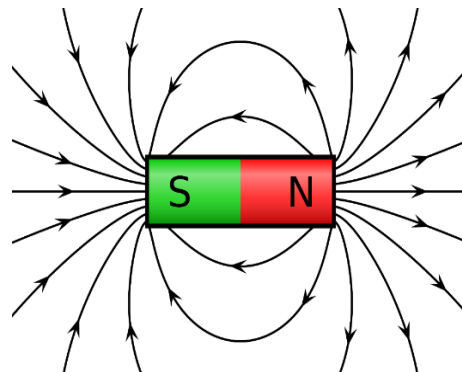


Figure 2-b- Represents the direction of the field at different points [10].

Basic Considerations and Equations

The main goal of studying the pulsars stars, is to maintain the behavior of those Unique stars for showing their strong magnetic field, beside the radiating signal that we have, reserved as pulses from this star and other factors, by taking the data of many pulsars period (P) and period derivative (\dot{P}) for both types of normal and millisecond and applying the suitable formulae mathematical equation and discuss their actions. In this work, the complementary model Ostriker and Gunn (1970) considered an inclined the Magnetic field with the rotational axis as shown in figure 3.

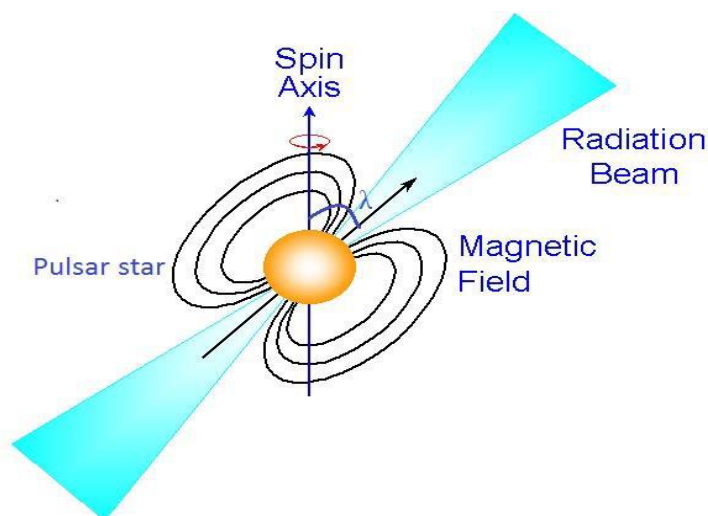


Figure 3- Represents Ostriker and Gunn Model

The main energy loss mechanism is due to the emission of magnetic dipole whose luminosity will be determined by the strength of the magnetic field.

The Magnetic Field and the Spin down Luminosity with pulsar's Period derivative.

Relations can estimate the surface Magnetic field of pulsars (Bs) as [12]:

$$Bs = (3.2)10^{-19} \sqrt{p\dot{p}} (G). \quad (1)$$

According to alven notation [12], the magnetic field is given by the relation:

$$Bs = \frac{a}{r^3} [1 + 3 \sin^2 \lambda]^{\frac{1}{2}} \quad (2)$$

Where λ is given by:

$$\lambda = \frac{1}{2} \pi - \theta$$

This relation represents the first approximation of the magnetic dipole.

The dipole moment of this field is [12,14]:

$$a = BR^3 \quad (3)$$

Where: P :Pulsar's period

\dot{p} : Pulsar's period derivative

B: the magnetic field induction produced a current density at some point.

λ : the latitude

r: is the vector that directed from point of integration

R: radius of pulsar.

θ : the angle between magnetic field axis and rotation axis

The Spin down Luminosity or Loss Rotation Energy (Lsp) mathematical equation as follow in (4) relation;

$$L_{sp} = 4\pi^2 I \dot{P} P^{-3} \text{ (erg/s)} \quad (4)$$

Where I= The pulsar's moment of inertia $\sim 10^{45} \text{ g cm}^2$

The heating rate (Eh) of pulsar can be find from equation (5),[11].

$$E_h = 4\pi^2 I f \dot{P} P^{-3} \text{ (erg/s)}. \quad (5)$$

Where f value is given by from equation (6);

$$f = E_h / E_{rot} = 1 + \frac{P}{P_m} \quad (6)$$

$$P_m \text{ value } \sim (1 \dots \dots 2)$$

In addition the relation (7) below can represent the Characteristic Age (τ_c);

$$\tau_c = P / 2 \dot{P} \text{ (years)} \quad (7)$$

The Rotation Energy of Pulsar star (Erot) is represent by equation (8).

$$E_{rote} = 4\pi^2 I f \dot{P} P \quad (8)$$

Moreover, the spin down age (T) estimated from the following equation [12]:

$$T = \frac{P}{\dot{P}} \quad (9)$$

The counting spinning times of pulsars around its axis is given by equation as [12]:

$$Spin = p * \dot{p} (\text{spins}) \quad (10)$$

Calculations and results

For gamma, x and optical normal pulsars.

The values and surface magnetic field were be calculated by using equation (1) as estimated in table 1 [13].

According to the relation that had been showed between (Bs) and (P) that, the (Bs) at the smallest amount of (P) goes to the maximum value after values of (Bs) less in sharply and that indicates that stars in those period are young and have a strong magnetic field.

After that sharpening decrement the (Bs) raise again gradually as the period increased as shown in figure 4.

Table 1- Represents the calculated values of surface magnetic field for adopted sample of normal pulsars are illustrate related to observation of period and derivative period [13].

PSR	COMMENT	Period (ms)[14]	$\dot{p} * 1.0e - 15$ ($s.s^{-1}$) [14]	$B * 1.0e + 13$ (G)
BO351+21	Crab	33.40	420.96	0.3794
B0833-45	Vela	89.29	124.67	0.3376
J0205+6449	3C58	65.67	193.52	0.3607
J2229+6114	G106.6+2.9	51.62	78.27	0.2034
J1617-5055	Near RCW 103	69.66	136.05	0.3115
B0633+17	Gemini	237.09	10.97	0.1632
B1706-44	In G3431-02.3	102.45	93.04	0.3124
B1509-58	In MSH 15052	150.23	1540.19	1.5393
B1951+32	In CTB 80	39.53	5.85	0.0487
J1930+1852	In G54.1+0.3	136.85	750.20	1.0253
J1811-1926	In G11.2-0.3	64.67	44	0.1707
B61046-58	Vela twin	123.65	95.92	0.3485
B1259-63	Be-star/bin-	47.79	2.27	0.0333
J0537-6909	In N157B/LMC	16.11	51.24	0.0919
J1420-6048		68.18	82.85	0.2405
B1823-13	Vela like	101.45	74.95	0.2790
B1800-21	G8.7-0.1	133.61	134.32	0.4287
B1929+10		226.51	1.16	0.0519
B0656+14	Cooling NS	384.87	55.03	0.4657
B0540-69	In N158A.LmC	50.39	479.06	0.4972
J1105-6107		63.19	15.80	0.1011
B0950+08		253.06	0.23	0.0244
B1610-50		231.60	492.54	1.0808
J058+2817	In G180.0-1.7	143.15	3.66	0.0732
B1055-52	Cooling NS	197.10	5.83	0.1085
B0355+54		156.38	4.39	0.0838
B2334+61	G114.3+0.3	495.24	191.91	0.9865
B0823+26		530.66	1.72	0.0967

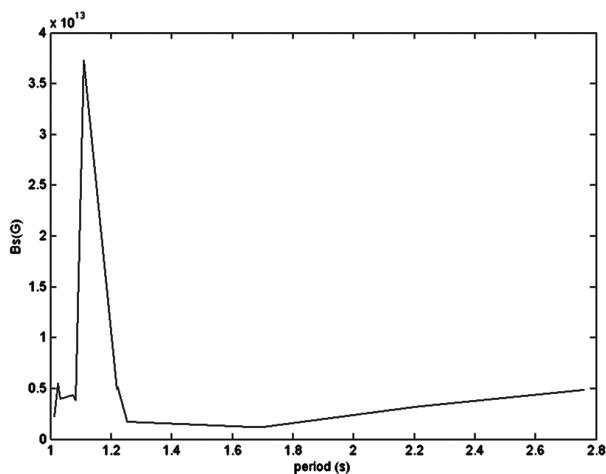


Figure 4- Represents the relation between surface magnetic field (Bs) and the period (p) for normal samples.

The spin down luminosity values calculated by using equation (4) as illustrated in table 2. Figure 5 showed the relation between the surface magnetic field (B_s) and the spin down luminosity (L_{sp}), as long as the surface magnetic field (B_s) increased the Spin down Luminosity (L_{sp}) increase too, from this leads to conclude that when the star has strong magnetic field (B_s) the value of Spin down Luminosity (L_{sp}) strong and that will increase the losing energy and go slow in rotation.

Table 2- Represents the calculation values of The Spin down Luminosity with respect to the surface magnetic field for normal samples.

PSR	$B_s \times 1.0e+13$ (G)	$L_{sp} \times 1.0e+34$ (erg/s)
BO351+21	0.3794	4.4603
B0833-45	0.3376	0.0691
J0205+6449	0.3607	0.2698
J2229+6114	0.2034	0.2246
J1617-5055	0.3115	0.1589
B0633+17	0.1632	0.0003
B1706-44	0.3124	0.0342
B1509-58	1.5393	0.1793
B1951+32	0.0487	0.0374
J1930+1852	1.0253	0.1156
J1811-1926	0.1707	0.0642
B61046-58	0.3485	0.0200
B1259-63	0.0333	0.0082
J0537-6909	0.0919	4.8382
J1420-6048	0.2405	0.1032
B1823-13	0.2790	0.0283
B1800-21	0.4287	0.0222
B1929+10	0.0519	0.00001
B0656+14	0.4657	0.0004
B0540-69	0.4972	1.4781
J1105-6107	0.1011	0.0247
B0950+08	0.0244	0.00001
B1610-50	1.0808	0.0157
J058+2817	0.0732	0.0005
B1055-52	0.1085	0.0003
B0355+54	0.0838	0.0005
B2334+61	0.9865	0.0006
B0823+26	530.66	1.72

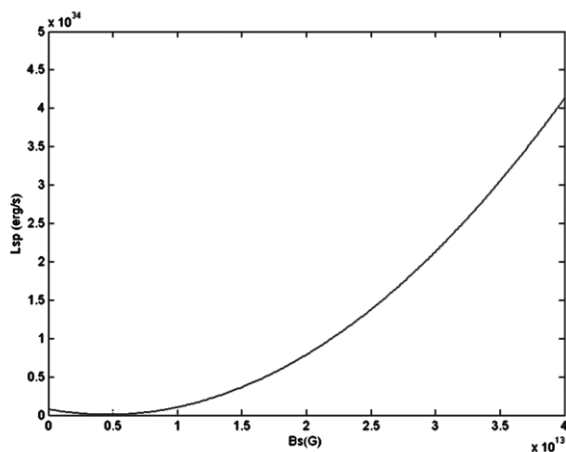


Figure 5- Represents the relation between The Spin down Luminosity and surface magnetic field for normal samples.

The values of heating rate (Eh) were be calculated by using equation (5) as illustrated in table 3.

Figure 6 showed that the heating rate (Eh) values increase with the magnetic field. This behavior due to the affecter of factor (f) in equation (6). This leads to the proving that the direction proportionality between the heating rate and star period.

Table 3- Represents the values of the period, surface magnetic field & heating rate for normal samples.

PSR	Period (ms)	B*1.0e+13 (G)	Eh*1.0e+36 (erg/s)
BO351+21	33.40	0.3794	4.2994
B0833-45	89.29	0.3376	0.0682
J0205+6449	65.67	0.3607	0.2647
J2229+6114	51.62	0.2034	0.2193
J1617-5055	69.66	0.3115	0.1561
B0633+17	237.09	0.1632	0.0003
B1706-44	102.45	0.3124	0.0337
B1509-58	150.23	1.5393	0.1779
B1951+32	39.53	0.0487	0.0198
J1930+1852	136.85	1.0253	0.0630
J1811-1926	64.67	0.1707	0.1145
B61046-58	123.65	0.3485	0.0362
B1259-63	47.79	0.0333	0.0080
J0537-6909	16.11	0.0919	4.4898
J1420-6048	68.18	0.2405	0.1013
B1823-13	101.45	0.2790	0.0280
B1800-21	133.61	0.4287	0.0220
B1929+10	226.51	0.0519	0.00001
B0656+14	384.87	0.4657	0.0004
B0540-69	50.39	0.4972	1.4424
J1105-6107	63.19	0.1011	0.0242
B0950+08	253.06	0.0244	0.00001
B1610-50	231.60	1.0808	0.0156
J058+2817	143.15	0.0732	0.0005
B1055-52	197.10	0.1085	0.0003
B0355+54	156.38	0.0838	0.0004
B2334+61	495.24	0.9865	0.0006
B0823+26	530.66	0.0967	0.00001

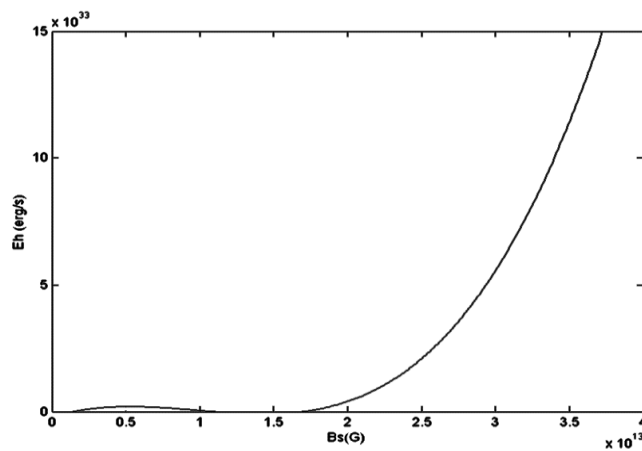


Figure 6- Represents the relation between the magnetic field and heating rate for normal samples.

The values of the Characteristic Age (τ_c) are calculated by using equation (7) as illustrated in table 4. The relation between the Characteristic Age (τ_c) and the period (P) is shown in figure 7. The results showed that the pulsars with period (1-3) s may be have maximum values of the Characteristic Age (τ_c). This due to the mechanism of losing energy of pulsars with these periods. Figure 7 showed that the relation between the Characteristic Age (τ_c) and the period (P) has the same behavior as the surface magnetic field (B_s) with the period (P).

Table 4- Represents the calculated values of the Characteristic Age with the period and period derivative for normal samples.

PSR	Period (ms)	$\dot{P} * 1.0e-15$ (s.s ⁻¹)	$\tau_c * 1.0e+10$ (years)
BO351+21	33.40	420.96	0.0004
B0833-45	89.29	124.67	0.0036
J0205+6449	65.67	193.52	0.0017
J2229+6114	51.62	78.27	0.0033
J1617-5055	69.66	136.05	0.0025
B0633+17	237.09	10.97	0.1081
B1706-44	102.45	93.04	0.0055
B1509-58	150.23	1540.19	0.0005
B1951+32	39.53	5.85	0.0338
J1930+1852	136.85	750.20	0.0009
J1811-1926	64.67	44	0.0073
B61046-58	123.65	95.92	0.0065
B1259-63	47.79	2.27	0.1052
J0537-6909	16.11	51.24	0.0016
J1420-6048	68.18	82.85	0.0041
B1823-13	101.45	74.95	0.0068
B1800-21	133.61	134.32	0.0050
B1929+10	226.51	1.16	0.9763
B0656+14	384.87	55.03	0.0350
B0540-69	50.39	479.06	0.0005
J1105-6107	63.19	15.80	0.0200
B0950+08	253.06	0.23	5.5013
B1610-50	231.60	492.54	0.0024
J058+2817	143.15	3.66	0.1956
B1055-52	197.10	5.83	0.1690
B0355+54	156.38	4.39	0.1781
B2334+61	495.24	191.91	0.0129
B0823+26	530.66	1.72	1.5426

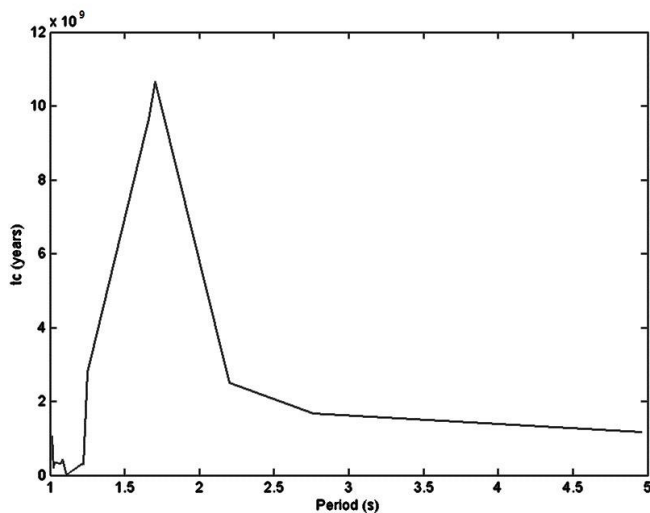


Figure 7- Represents the relation between the period and the Characteristic Age for normal samples.

Finally, the relation between the spin down luminosity and the spins of pulsar to obtain the losing energy of pulsar as follow in figure 8.

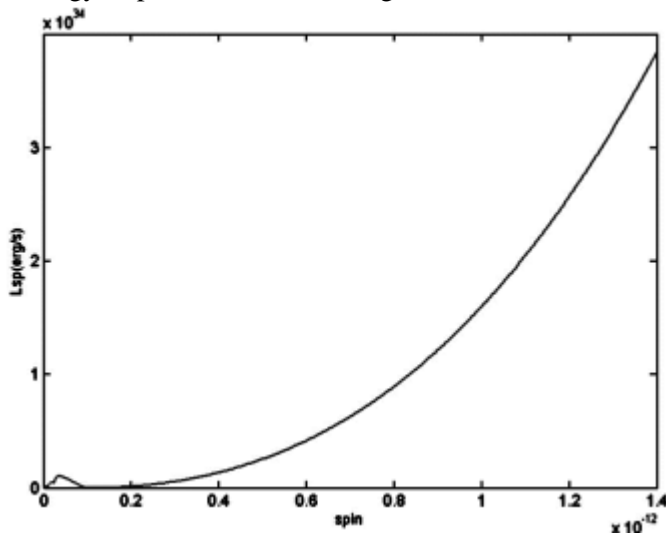


Figure 8- Represents the relation between spin and spin down luminosity form normal samples.

As noticed from figure 8, as long as the spins increases the spin down luminosity increases too, so from this this figure indicates the losing energy from the spinning motion of the star around its axis.

For gamma, x and optical MSP Pulsars.

Table 5 illustrates the calculated values of (Bs) for MSP samples, which adopted at different values of period and period derivative by equation (1) as [14]. Figure 9 shows the relation between (Bs) and the period (P) is the (Bs), this figure shows as the period (P) of star increase the surface magnetic field (Bs) increase too but in smooth increasing unlike the normal pulsars of the same relation.

Table 5- Represents the calculated values of surface magnetic field for adopted sample of MSP pulsars are illustrate related to observation of period and derivative period [14].

Name	Comment	Period (ms)	$P \cdot 1.0e-15 \text{ SS}^{-1}$	$B \cdot 1.0e+9 \text{ (G)}$
J0437-4715	Bin	5.75	$2 \cdot 10^{-5}$	0.3432
B1937+21	Sol	1.55	$1 \cdot 10^{-4}$	0.3984
B1821-24	Sol.M28	3.05	$1.6 \cdot 10^{-3}$	2.2354
J0030+0451	Sol	4.86	$1 \cdot 10^{-5}$	0.2231
J2124-3358	Sol	4.93	$1.1 \cdot 10^{-5}$	0.2357
B1957+20	Bin	1.60	$1.2 \cdot 10^{-5}$	0.1402
J1024-0719	Sol	5.18	$1.8 \cdot 10^{-5}$	0.3090
J1744-1134	Bin	4.07	$8.6 \cdot 10^{-6}$	0.1893
J1012+5307	Bin	5.25	$1.4 \cdot 10^{-5}$	0.2743
J0218+4232	Bin	2.32	$8 \cdot 10^{-5}$	0.4360
J0751+1807	Bin	3.47	$8 \cdot 10^{-5}$	0.5332
J0024-7205E	Bin, 47Tue	3.53	$3 \cdot 10^{-4}$	1.0414
JJ0024-7504F	Sol, 47Tue	2.63	$2.1 \cdot 10^{-4}$	0.7520
0024-7203J	Bin, 74Tue	2.10	$1.1 \cdot 10^{-4}$	0.4864
0024-7204O	Bin, 74Tue	2.64	$1.8 \cdot 10^{-4}$	0.6976
0024-7203U	Bin, 74Tue	4.34	$3.4 \cdot 10^{-4}$	1.2292
0024-7204N	Sol, 74Tue	3.05	$1.5 \cdot 10^{-4}$	0.6845
J0024-7204I	Bin, 74Tue	3.48	$1.5 \cdot 10^{-4}$	0.7311
J0024-7204G	Sol, 74Tue	4.04	$1.9 \cdot 10^{-4}$	0.8866
J0024-7204D	Sol, 74Tue	5.75	$3 \cdot 10^{-4}$	1.3291
J0023-7205M	Sol, 74Tue	3.67	$1.7 \cdot 10^{-4}$	0.7993
J0024-7204H	Bin, 74Tue	3.21	$1.8 \cdot 10^{-4}$	0.7692

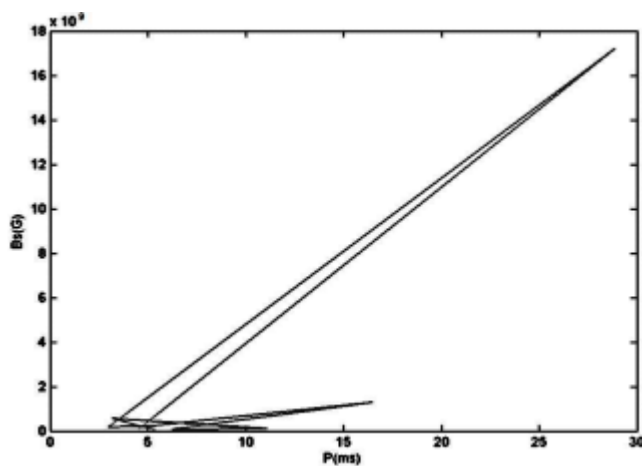


Figure 9- Represents the relation between surface magnetic field (Bs) and the period (p) for MSP

The calculated values of the spin down luminosity (L_{ps}) from equation (4) are given in table 6.

Table 6 illustrates that the values of (L_{sp}) of MSP is less than the values in the normal pulsar. The relation between (B_s) and (L_{sp}) shows a big rising as ($(0 - 2 \cdot 10^{10} \text{ G})$) in the first interval, which indicates high losing energy from the continuous rotation, after that the (L_{sp}) start to rise up gradually like the behavior of Normal as shown in figure 10.

Table 6- Represents the calculated values of The Spin down Luminosity with respect to the surface magnetic field of MSP samples.

Name	B*1.0e+9* (G)	Lsp*1.0e+28 (erg/s)
J0437-4715	0.3432	0.0042
B1937+21	0.3984	1.0601
B1821-24	2.2354	2.2263
J0030+0451	0.2231	0.0034
J2124-3358	0.2357	0.0036
B1957+20	0.1402	0.1157
J1024-0719	0.3090	0.0051
J1744-1134	0.1893	0.0050
J1012+5307	0.2743	0.0038
J0218+4232	0.4360	0.2529
J0751+1807	0.5332	0.0756
J0024-7205E	1.0414	0.2693
JJ0024-7504F	0.7520	0.4557
0024-7203J	0.4864	0.4689
0024-7204O	0.6976	0.3862
0024-7203U	1.2292	0.1642
0024-7204N	0.6845	0.2087
J0024-7204I	0.7311	0.1405
J0024-7204G	0.8866	0.1138
J0024-7204D	1.3291	0.0623
J0023-7205M	0.7993	0.1358
J0024-7204H	0.7692	0.2148

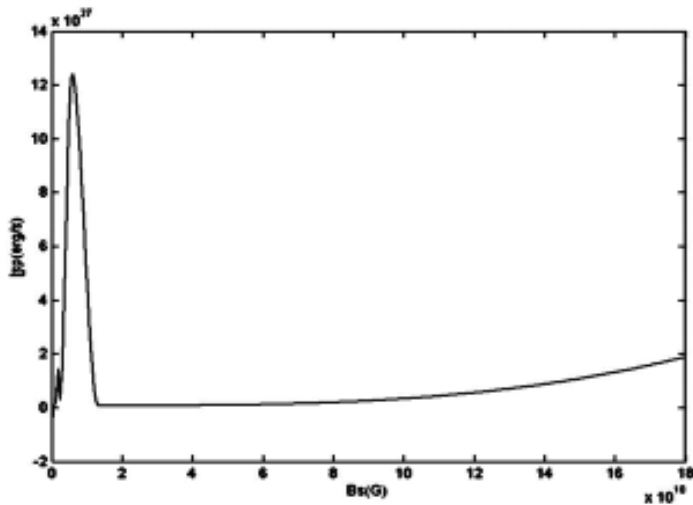


Figure 10- Represents the relation between The Spin down Luminosity and surface magnetic field for MSP samples.

Table 7 shows the calculated values of heating rate (Eh) for MSP by equation (5). To study the more about MSP's behavior and compare it with Normal samples, the figure 11 shows the relation between (Bs) and (Eh), and as noticed the same behavior as in figure 6 which explain the losing energy because of the age and the speed rotation.

Table 7- Represents the values of the period, surface magnetic field & heating rate for MSP samples.

Name	$B \cdot 1.0e+9^*$ (G)	$Eh \cdot 1.0e+28$ (erg/s)
J0437-4715	0.3432	0.0034
B1937+21	0.3984	0.5869
B1821-24	2.2354	1.5791
J0030+0451	0.2231	0.0027
J2124-3358	0.2357	0.0029
B1957+20	0.1402	0.0649
J1024-0719	0.3090	0.0041
J1744-1134	0.1893	0.0039
J1012+5307	0.2743	0.0031
J0218+4232	0.4360	0.1644
J0751+1807	0.5332	0.0556
J0024-7205E	1.0414	0.1988
JJ0024-7504F	0.7520	0.3089
0024-7203J	0.4864	0.2939
0024-7204O	0.6976	0.2621
0024-7203U	1.2292	0.1275
0024-7204N	0.6845	0.1480
J0024-7204I	0.7311	0.1034
J0024-7204G	0.8866	0.0869
J0024-7204D	1.3291	0.0512

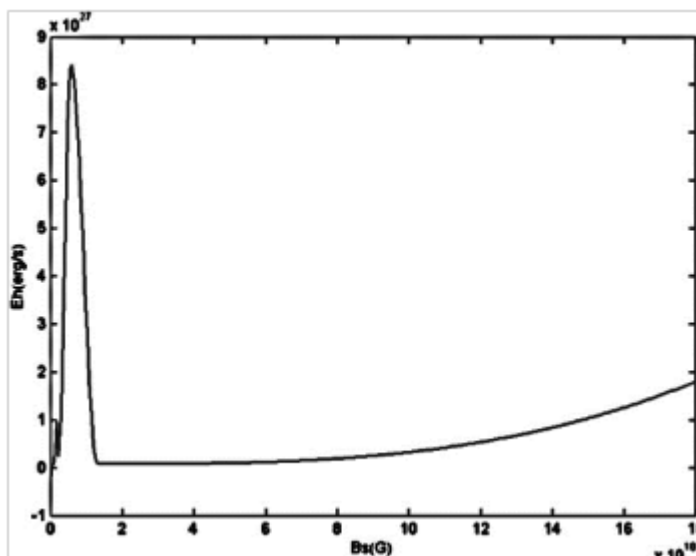


Figure 11- Represents the relation between the magnetic field and heating rate for MSP samples.

Table 8 represent the calculation of Characteristic Age (τ_c) of MSP's sample by equation (7). The relation between Period (P) and the Characteristic Age (τ_c) was illustrated in figure 12. The pulsars with periods (5-15) s have large Characteristic Age (τ_c) as in the figure 12 and shows the same behavior as in the Normal pulsars but the MSP is older than the normal due the fast rotation and the mechanism of rotation.

Table 8- Represents the calculated values of the Characteristic Age and with the period and period derivative for MSP samples.

Name	Period (ms)	$P \cdot 1.0e-15$ SS ⁻¹	$\tau c \cdot 1.0e+12$ (years)
J0437-4715	5.75	$2 \cdot 10^{-5}$	1.4375
B1937+21	1.55	$1 \cdot 10^{-4}$	0.0775
B1821-24	3.05	$1.6 \cdot 10^{-3}$	0.0095
J0030+0451	4.86	$1 \cdot 10^{-5}$	2.4300
J2124-3358	4.93	$1.1 \cdot 10^{-5}$	2.2409
B1957+20	1.60	$1.2 \cdot 10^{-5}$	0.6667
J1024-0719	5.18	$1.8 \cdot 10^{-5}$	1.4389
J1744-1134	4.07	$8.6 \cdot 10^{-6}$	2.3663
J1012+5307	5.25	$1.4 \cdot 10^{-5}$	1.8750
J0218+4232	2.32	$8 \cdot 10^{-5}$	0.1450
J0751+1807	3.47	$8 \cdot 10^{-5}$	0.2169
J0024-7205E	3.53	$3 \cdot 10^{-4}$	0.0588
JJ0024-7504F	2.63	$2.1 \cdot 10^{-4}$	0.0626
0024-7203J	2.10	$1.1 \cdot 10^{-4}$	0.0955
0024-7204O	2.64	$1.8 \cdot 10^{-4}$	0.0733
0024-7203U	4.34	$3.4 \cdot 10^{-4}$	0.0638
0024-7204N	3.05	$1.5 \cdot 10^{-4}$	0.1017
J0024-7204I	3.48	$1.5 \cdot 10^{-4}$	0.1160
J0024-7204G	4.04	$1.9 \cdot 10^{-4}$	0.1063
J0024-7204D	5.75	$3 \cdot 10^{-4}$	0.0958
J0023-7205M	3.67	$1.7 \cdot 10^{-4}$	0.1079

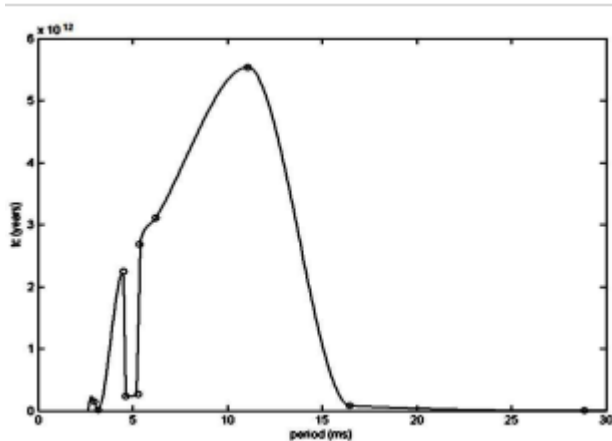


Figure 12- Represents the relation between the period and the Characteristic Age for MSP samples.

Conclusions

- The older Millisecond pulsars defined as having greater ages because P/\dot{P} specifies how long pulsar lives at that age.
- The results indicated that luminosity of pulsars must decline with age, also the luminosity must also depends upon some negative power of period.
- The maximum values of M.F strength will be at high values of period for pulsars.
- The heating rate will decrease with age that's due to the main energy loss mechanism is M.F radiation.

References

1. Bulent K, Athanasios K, Stephen E. 2010. *The Neutron Star Mass Distribution*, Thorsett, P. 23.
2. Young R. 2006. *Calculating a Neutron Star's Density*, Astronomical Society,
3. P.12, http://imagine.gsfc.nasa.gov/docs/science/know_12/black_holes.html

4. Joeri L. **2012**, *Neutron stars and pulsars: challenges and opportunities after 80 years*, Stronomical Union Symposium No. 291, P .71.
5. Werner B. **2009**, *Neutron Stars and Pulsars*, the Astrophysical Journal, P.75.
6. Kramer M, Wielebinske R. **2001**, "Gamma-ray Pulsars", *amer Astr. Sco. Astrophys Journal* .526, PP: 957-975.
7. Becker W. **2008**, *Neutron Stars and Pulsars*, Space Sci. Library. 357, PP.112.
8. Backer M, Davic V, **1982**.Nature .25.
9. Atkinson N. **2008**. Fermi Telescope Makes First Big Discovery: *Gamma Ray Pulsar*. Universe Today, P.33.
10. Harding A, Julie V, Dyks J, Frackowiak M. **2008**, High-Altitude Emission from Pulsar Slot Gaps: The Crab Pulsar, *The Astrophysical Journal*, 680(2), PP: 1378-1393.
11. Harding A, Grenier I, Gonthier P. **2007**, The *Geminga fraction*, Astrophysics and Space Science, Volume 309, Issue 1-4, P 221-230.
12. Lyne G, Manchester N, Lorimer R, Bailes , D'Amico N, Tauris T, Johnston S, Bell F, Nicastro L. **2010**, *The Parkes Southern Pulsar Survey - II. Final results and population analysis*, Monthly Notices of the Royal Astronomical Society, Volume 295, Issue 4, p. 743-755, 1998. Monthly Notices of the Royal Astronomical Society, Volume 295, Issue 4, P 743-755.
13. Lamb C, Macomb J. **1997**, *Point Sources of GeV Gamma Rays*, Astrophysical Journal v.488, P.87.
14. Camilo F, Manchester R, Gaensler M, Lorimer R, Sarkissian J. **2002**, PSR J1124-5916: Discovery of a Young Energetic Pulsar in the Supernova Remnant G292.0+1.8, *The Astrophysical Journal*, 567(1) PP. 71-75.